August 27-31, 2023
FLORENCE - ITALY
16th International Conference on Wind Engineering

Capacity assessment of transmission tower-line system subjected to the combined wind and ice loading

M.Y. Xiao [1], H.P. Hong [2]

[1]*Department of Civil and Environmental Engineering, University of Western Ontario, London, Ontario N6A 5B9, Canada, Email: mxiao44@uwo.ca*
[2]*Department of Civil and Environmental Engineering, University of Western Ontario, London, Ontario N6A 5B9, Canada, Email: hongh@eng.uwo.ca*

SUMMARY:
Assessment of the capacity of the transmission tower-line system subjected to the wind and ice accretion load is carried out in the present study. Analyses are carried out using an implemented finite element model of the tower-line system by using the incremental dynamic analysis (IDA) and the nonlinear static pushover analysis (NSPA). Results of the analysis indicate that the consideration of local buckling could be important to evaluate the capacity of the tower-line system subjected to the combined load. Failure of such a system subjected to the combined load initiates near the bottom of the tower or the cross-arm depending on the amount of ice load. Results indicate that the capacity curve obtained from NSPA agrees well with that obtained by using IDA; the capacity curve is sensitive to the orientation of the shape of the accreted ice to the incoming wind. This observation facilitates the development of the fragility curve.

Keywords: transmission tower, structural reliability, wind, and ice load

1. INTRODUCTION

Failure of transmission tower-line systems subjected to the combined wind and ice load has been reported. However, the capacity of the tower-line system subjected to such loading is rarely investigated by considering nonlinear inelastic behaviour, although it is noted that investigation of the tower capacity subjected to wind load has been extensively reported (Savory et al. 2001; Banik et al. 2010; Zhang et al. 2013; Mara and Hong 2013; Yang and Hong 2016; Yang et al. 2017; Fu et al. 2019; Tapia-Hernandez and De-Leon-Escobedo 2021; Zheng and Fan 2022). Yang et al. (2017) showed that the capacity of the tower-line system subjected to wind loading that is obtained by nonlinear static pushover analysis (NSPA) agrees well with that obtained by the incremental dynamic analysis (IDA). Moreover, Fu et al. (2019) showed that the use of several beam elements to model a structural member could cope with the effect of local buckling. Chen et al. (2019) studied the buckling capacity of the transmission tower under the simultaneous action of ice and wind load without considering the variation of the wind pressure coefficient caused by the accreted ice on the cable. Xie and Sun (2012) conducted tests to study the failure mechanism of two scaled sub-assemblages near the tower waist under ice and wind load. However, capacity evaluation of the tower-line system subjected to combined wind and ice load with the angle of attack dependent aerodynamic coefficient for iced cable has not been carried out. Also, it is unknown if the capacity curve of the tower-line system subjected to combined wind and ice load obtained by using

NSPA approximates well that obtained by using IDA.

The main objective of the present study is to assess the capacity of the tower-line system subjected to combined wind and ice load by using NSPA and IDA. In the following, we described the modelling of the tower-line system, wind and ice loading, analysis procedure, and obtained results.

2. MODELLING OF TOWER-LINE SYSTEM AND WIND AND ICE LOADING

A tower-line system consisting of a self-supported lattice transmission tower and 2 spans of conductors is modelled using ANSYS as illustrated in Figure 1. The geometric variables and material properties of the tower-line system are the same as those used by Mara and Hong (2013). The bilinear model is used to represent the material nonlinear behavior of the tower members. The ratio of post-yield stiffness to initial stiffness equals 0.05. A damping ratio of 0.02 is used in the analysis. The connection between structural elements is assumed to be rigid. However, unlike Mara and Hong (2013), each structural element is represented by 3 2-node 3-dimension beam elements to cope with possible local buckling effects.

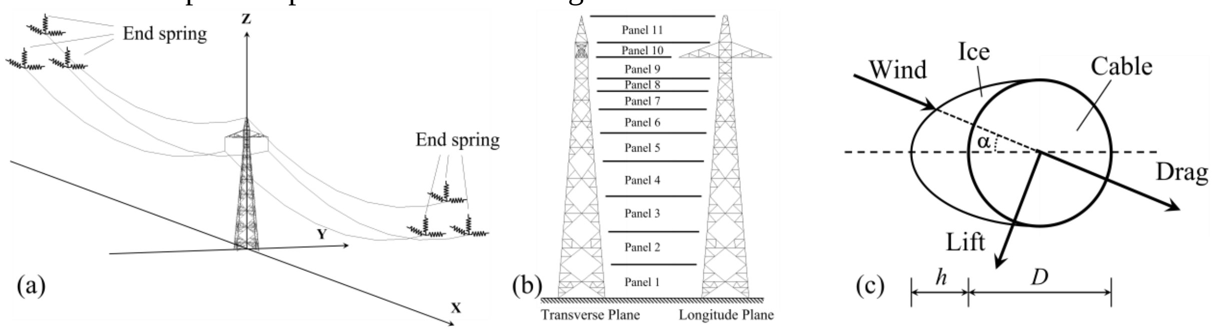

Figure 1. *a*) Three-dimension isometric view of transmission tower-line system, *b*) Definition of wind load panels, and *c*) Illustration of ice accretion geometry.

The span length between towers is 488 meters. For multi-span tower-line systems, the sag-to-span ratio of cables is set equal to 0.03 and the initial geometric shape of the conductors, each modelled using 30 link elements, is determined as was done by Yang and Hong (2016). Also, the same damping ratio for the cables and the equivalent stiffness for the end cables K_e (kN/m) given in Yang et al. (2017) are adopted.

The mean speed along the height is assumed to follow the power law with the exponent equal to 0.16. The adopted power spectrum density (PSD) function (i.e., Kaimal spectrum) of the turbulent wind $S_V(f, \boldsymbol{p})$ is,

$$S_V\left(f,\boldsymbol{p}\right)=\sigma_V^2(100z/V_{mean}(x,z))/\left[3(1+50f_V(x,z))^{5/3}\right] \tag{1}$$

where $\boldsymbol{p} = (x, z)$ denotes the spatial location; σ_V is the standard deviation of the fluctuating wind speed which equals $0.1\times V_{mean}(x,z)$; f (Hz) is the frequency; $f_V(x,z) = fz/V_{mean}(x,z)$, and $V_{mean}(x,z)$ is the mean wind speed. We adopt Davenport's coherence model with the exponential decay coefficients equal to 16 along the x-axis and 10 along the z-axis. The simulation of the vector of the fluctuating wind speed $v_j(t)$ at $\boldsymbol{p}_j$ is carried out using the spectral representation method (SRM) (Shinozuka and Jan 1972). Sampled winds will be used for IDA analysis in the following section.

The evaluation of the wind load is carried out according to CAN/CSA C22.3 (CSA 2010) by dividing the tower into 11 panels as shown in Figure 1b. The calculated wind load is distributed among all the nodes within the considered panel. For ice-covered cables, the aerodynamic coefficient suggested by Li et al. (2019) is adopted, and the considered ice accretion shape on the cable as well as the definition of geometrical variables are illustrated in Figure 1c.

3. CAPACITY ASSESSMENT ANALYSIS

First, capacity assessment of the tower-line system subjected to combined wind and ice loading is carried out using the NSPA by considering that the mean wind is perpendicular to the transmission line (i.e., along the y-axis, see Figure 1*a*), $B=h/D$ equals 0.2 and 1.0 and, the angle of attack shown in Figure 1c equals 90°. In the present study, NSPA is carried out through the transient analysis with an increasing rate of wind speed of 0.1 m/s per 10 seconds. The obtained deformed shape and typical failure mechanisms are shown in Figure 2.

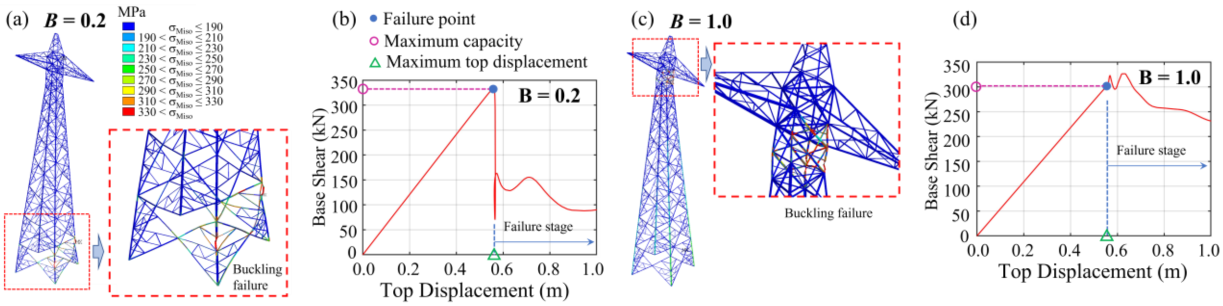

Figure 2. Failure mechanism and capacity curve are shown in *a*) and *b*) for B = 0.2, *c*) and *d*) for B = 1.

As can be observed from the figure, the location where failure initiates depends on the B value. The failure starts near the bottom of the tower for B = 0.2 which is similar to the case under wind loading alone. The initial failure occurs near the cross-arm for B = 1.0. This can be explained by noting that as B (i.e., ice accretion loading) increases the gravity load and wind load acting on the cable increase. In all cases, the capacity curves indicate that the tower-line system fails in an almost brittle manner, which is unlike the capacity curves shown in some of the previous studies for this type of structure. To investigate this, we considered that each structural member is represented by a single beam element, rather than 3 beam elements. In such a case, the obtained capacity curves exhibit a smooth transmission from yield to ultimate capacity. This indicates the importance to model a structural member with multiple beam elements to capture the local buckling effect.

As the considered structure with the ice loading could be wind-sensitive, structural analysis for the setting considered for Figure 1 is carried out again but using the IDA. By using the obtained results for 25 simulated spatially varying winds, each with a duration of 1 minute, the obtained capacity curve in terms of the (peak) temporal-averaged gust wind speed $v_{p\tau}$, with τ = 3 or 10 s, versus drift ratio is shown in Figures 3*a* to 3*f*, where the vertical axis represents $v_{p\tau}$ and the horizontal axis represents the maximum tip drift ratio. The variability of the capacity curves reflects the record-to-record variability. The use of $v_{p\tau}$ versus drift ratio facilities the reliability analysis (Yang et al. 2017) since the probabilistic wind hazard assessment is often carried out in terms of 10-min or hourly mean wind speed – such a wind speed can be converted to $v_{p\tau}$. For comparison purposes, the capacity curves obtained based on NSPA shown in Figure 2 are also presented in Figures 3*a* to 3*f*, where $v_{p\tau}$ for the capacity curve is assumed to be equal to the wind speed that leads to the required base shear obtained using NSPA v_{eq}. The comparison indicates that the capacities obtained by using NSPA agree well with those obtained based on IDA. The results also show that v_{eq} could be used as $v_{p\tau}$, where τ equals 3 or 10 s. The analysis that is carried out for the results presented in Figure 2 and Figures 3*a* to 3*f* is repeated but for the angle of attack equal to 40°. To save space, these results are not plotted. However, a comparison of the results by considering α = 40° indicates that the observations for α = 90° are equally applicable for those obtained for α = 40°, except that the maximum load-carrying capacity decreases as the angle of attack varies from 90° to 40°.

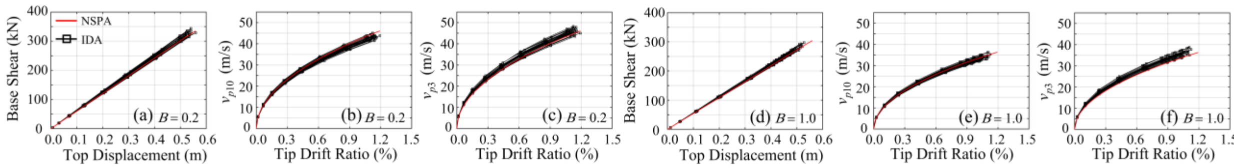

Figure 3. Effect of proportion of ice load on the capacity curve obtained by IDA and NSPA. *a*) to *c*) are for *B* = 0.2, and *d*) to *f*) are for *B* = 1.

4. CONCLUSIONS

An analysis of the capacity of the transmission tower-line system is carried out. The analysis results indicate that the capacity curve obtained by using NSPA agrees well with that obtained by using IDA. Results also indicate that the consideration of local buckling can affect the assessed capacity curve and that the capacity curve is sensitive to the angle of attack (see Figure 1c).

ACKNOWLEDGEMENTS

The financial support received from the China Scholarship Council (No. 201807980004, for MYX) and the Natural Sciences and Engineering Research Council of Canada (RGPIN-2016-04814, for HPH) is gratefully acknowledged.

REFERENCES

Banik, S. S., Hong, H. P., and Kopp, G. A., 2010. Assessment of capacity curves for transmission line towers under wind loading. Wind and Structures 13(1), 1-20.

Chen, J., Xian, Q., and Zhang, P., 2019. Buckling Analysis of Transmission Tower Considering Ice Load. In IOP Conference Series: Materials Science and Engineering, Sept. 2019. IOP Publishing, 012036.

CSA (Canadian Standards Association), 2010. Design criteria of overhead transmission lines. CAN/CSA-C22.3 No. 60826-10, Toronto.

Fu, X., Wang, J., Li, H. N., Li, J. X., and Yang, L. D., 2019. Full-scale test and its numerical simulation of a transmission tower under extreme wind loads. J. of Wind Engineering and Industrial Aerodynamics 190, 119-133.

Li, J. X., Fu, X., and Li, H. N., 2019. Experimental study on aerodynamic characteristics of conductors covered with crescent-shaped ice. Wind and Structures 29(4), 225-234.

Mara, T. G. and Hong, H. P., 2013. Effect of wind direction on the response and capacity surface of a transmission tower. Engineering Structures 57, 493-501.

Savory, E., Parke, G. A., Zeinoddini, M., Toy, N., and Disney, P., 2001. Modelling of tornado and microburst-induced wind loading and failure of a lattice transmission tower. Engineering Structures 23(4), 365-375.

Shinozuka, M. and Jan, C. M., 1972. Digital simulation of random processes and its applications. Journal of sound and vibration, 25(1), 111-128.

Tapia-Hernández, E. and De-León-Escobedo, D., 2021. Vulnerability of transmission towers under intense wind loads. Structure and Infrastructure Engineering, 1-16.

Xie, Q. and Sun, L., 2012. Failure mechanism and retrofitting strategy of transmission tower structures under ice load. Journal of Constructional Steel Research 74, 26-36.

Yang, S. C. and Hong, H. P., 2016. Nonlinear inelastic responses of transmission tower-line system under downburst wind. Engineering Structures 123, 490-500.

Yang, S. C., Liu, T. J., and Hong, H. P., 2017. Reliability of tower and tower-line systems under spatiotemporally varying wind or earthquake loads. Journal of Structural Engineering 143(10), 04017137.

Zhang, Z., Li, H., Li, G., Wang, W., and Tian, L., 2013. The numerical analysis of transmission tower-line system wind-induced collapsed performance. Mathematical Problems in Engineering 2013.

Zheng, H. D. and Fan, J., 2022. Progressive collapse analysis of a truss transmission tower-line system subjected to downburst loading. Journal of Constructional Steel Research 188, 107044.